Cement and Concrete Research 40 (2010) 45–57

Contents lists available at ScienceDirect

Cement and Concrete Research

journal homepage: http://ees.elsevier.com/CEMCON/default.asp

Fundamental mechanisms for polycarboxylate intercalation into C_3A hydrate phases and the role of sulfate present in cement

Johann Plank [*], Dai Zhimin, Helena Keller, Friedrich v. Hössle, Wolfgang Seidl

Department of Chemistry, Technische Universität München, Garching, Germany

A R T I C L E   I N F O

Article history:
Received 7 May 2008
Accepted 19 August 2009

Keywords:
Cement (D)
Polymers (D)
Concrete (E)
Admixture (D)
Organo-mineral phase

A B S T R A C T

The fundamental reactions leading to the intercalation of polycarboxylate (PC) superplasticizers into calcium aluminum hydrates were studied by hydration of pure C_3A in the presence of PC at 75 °C. It was found that the amount of dissolved sulfate present in cement pore solution determines whether organo-mineral phases are formed or not. In the absence of sulfate, PCs easily intercalate during C_3A hydration in alkaline solution. Under these conditions, only excessive steric size of the PC will prevent intercalation. At low sulfate concentrations (SO_4^{2-}/C_3A molar ratios of 0.1–0.35), PC intercalates with intersalated alkali sulfate, are formed. At high sulfate concentrations (SO_4^{2-}/C_3A molar ratios of 0.7–2), PC can no longer intercalate. Instead, sulfate, because of its higher negative charge density, fills the interlayer space and monosulfoaluminates with different water contents are formed.

Anion exchange experiments confirm that from the initially formed C_4AH_{13}, PC will exchange the interlayer OH^- anion whereas with monosulfoaluminates, no replacement of sulfate by PC was found. Consequently, in alkaline solution, PC intercalates will not exchange their PC against OH^- anions whereas sulfate will gradually replace the PC.

Generally, intercalation of PC is an unwanted process because it consumes superplasticizer which is effective only when it adsorbs onto the cationic surfaces of AF_m and AF_t phases. Our experiments demonstrate that intercalation can be avoided by using PCs with long side chains or highly sulfated cements (SO_4^{2-}/C_3A molar ratio ≥ 0.75) containing alkali or calcium sulfates which dissolve fast. In undersulfated cements, however, PC intercalates can be formed, either directly during the stacking process of the $[Ca_2Al(OH)_6]^+$ main layer, with PC acting as the template which determines the interlayer distance, or by anion exchange between initially formed aluminate hydrates (e.g. C_4AH_{13} or C_2AH_8) and the PC anion.

1. Introduction

Polycarboxylate-based superplasticizers (PCs) are recognized as important admixtures for use in modern concrete technology [1]. They allow the production of a highly flowable concrete or to reduce the water to cement ratio of concrete, resulting in higher compressive strength. For optimum use, it is essential to profoundly understand all potential ways of interaction between PCs and the mineral compounds formed during cement hydration. It has been generally accepted that the high range water reduction and the high fluidity of concrete containing PC is attributed to the PCs adsorbing onto the surface of cement hydrate phases [2]. Thus, a layer exercising a steric effect is formed which leads to the dispersion of the cement particles [3–6]. The hydration of tricalcium aluminate (C_3A) and tetracalcium alumoferrite (C_4AF) present in cement can produce hydrocalumite-type layered double hydroxides (LDHs) which have the potential to intercalate various anions between the cationic main layers.

C_3A accounts for approx. 5–10% of the clinker mass of ordinary Portland cement (OPC). During its hydration, the layered phases C_2AH_8 and C_4AH_{13} which belong to the family of calcium aluminum layered double hydroxides (Ca–Al–LDHs), are initially formed as metastable compounds [7,8]. They contain hydroxide as interlayer anion. Depending on temperature, they convert within minutes or hours to the cubic katoite phase C_3AH_6 which is the most stable calcium aluminate hydrate at room temperature. Sulfate, e.g. in the form of gypsum which is commonly present in any OPC to control its setting behavior, can intercalate into the layered calcium aluminate hydrates as well, resulting in $[Ca_4Al_2(OH)_{12}](SO_4)\cdot 6\ H_2O$, or monosulfoaluminate which is also called AF_m phase [9]. Its interlayer is occupied by sulfate anions and water molecules. β-Naphthalene sulfonate (BNS) formaldehyde condensate, a linear unbranched polymer commonly used as superplasticizer, was the first concrete admixture for which intercalation into calcium aluminate hydrate phases has been experimentally confirmed [10]. Also, novel hybrid LDH materials incorporating arene sulfonates such as nitrobenzoic acid, naphthalene-2,6-disulfonic acid

---

[*] Corresponding author. Tel.: +49 89 289 13151; fax: +49 89 289 13152.
E-mail address: johann.plank@bauchemie.ch.tum.de (J. Plank).

0008-8846/$ – see front matter © 2009 Elsevier Ltd. All rights reserved.
doi:10.1016/j.cemconres.2009.08.013

and naphthalene-2 sulfonic acid have been reported [11]. Recently, we described the intercalation of comb-type PC superplasticizers into calcium aluminum layered double hydroxides formed during the hydration of C_3A in the absence of sulfate [12,13].

Generally, LDHs are host–guest materials consisting of positively charged metal oxide/hydroxide sheets with intercalated anions and water molecules. Their general composition can be expressed by the formula $[M^{II}_{1-x} M^{III}_{x} (OH)_2]^{x+} [A^{n-}_{x/n}] \cdot z\, H_2O$, where M^{II} and M^{III} represent metal cations and A^{n-} the interlayer anion. Allmann and Brown et al. were the first to elucidate the structure of LDHs [14,15]. A schematic illustration of the lamellar structure of Ca–Al–A–LDH is shown in Fig. 1. The steric size and orientation of the anions intercalated between the main layers determine the interlayer distance. The *001* reflection shown in the X-ray powder diffractograms of these compounds allows one to calculate the basal spacing d between the main layers.

Owing to the highly tunable LDH main layer and interlayer composition coupled with a wide possible choice of organic anions, a large variety of LDH hybrid materials has been reported. Various kinds of polymers such as linear polymers, poly(ethylene oxide) derivatives [16], poly(α,β-aspartate) [17], poly(acrylic acid), poly(vinyl sulfonate), poly(styrene sulfonate) [18] and bimolecular DNA [19] have been intercalated between double hydroxide layers. The formation of these hybrid materials may proceed via different pathways such as coprecipitation, anion exchange, surfactant-mediated incorporation, rehydration, or restacking.

In this study, we investigated potential mechanisms of PC incorporation into calcium aluminate hydrates formed during early cement hydration. It is important to understand these potential processes because intercalation reduces the amount of PC available for adsorption and thus decreases its dispersing power. Out of all potential formation processes for LDH compounds mentioned above, rehydration of C_3A and anion exchange between AF_m phases and PC may occur during early cement hydration. Therefore, these two processes were chosen for the study. Coprecipitation was not investigated because of the low concentration of Al^{3+} commonly present in cement pore solution (0.2–0.3 µm/L). Thus, it was concluded that in industrial cements, this potential route of PC intercalation will not be significant. First, the ability of PC to intercalate as a function of its steric size (side chain length) was investigated. Then, C_3A (re)hydration experiments were carried out in presence and absence of PC and with varying amounts of sulfate, representing cements with different ratios between C_3A and sulfate. Finally, anion exchange reactions between PC intercalates and OH^- and SO_4^{2-}, resp., as well as between monosulfoaluminate and C_4AH_{13}, resp. and PC were performed. Our goal was to gain an understanding of conditions favorable for PC intercalation and to develop a scheme of potential reaction patterns involved in the intercalation of PCs into cement hydrate phases.

2. Experimental

2.1. Materials and methods

Pure tricalcium aluminate (C_3A) was synthesized via a sol–gel process followed by calcination of the gel for 14 h at 1260 °C with intermediate grindings [20]. Analysis by X-ray powder diffraction confirmed the resulting product to be pure tricalcium aluminate.

The Ca–Al–A–LDH-phases ($A = SO_4^{2-}$ or OH^-) described in the following were synthesized from freshly prepared calcium oxide obtained by calcination of calcium carbonate for 12 h at 950 °C (p.a., Merck). Additional raw materials were aluminum hydroxide (p.a., Merck), gypsum (p.a., Merck) and C_3A.

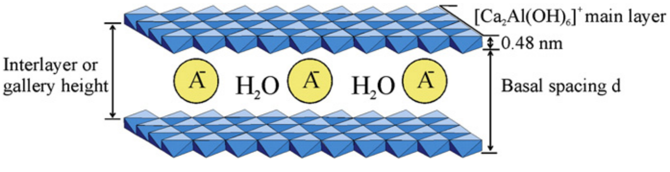

Fig. 1. Schematic illustration of the lamellar Ca–Al–A–LDH structure ($A^- =$ anion).

Monosulfoaluminate, $[Ca_4Al_2(OH)_{12}](SO_4) \cdot 12\, H_2O$ was synthesized according to a patent [21]. 13.46 g calcium oxide (0.24 mol), 12.48 g aluminum hydroxide (0.16 mol) and 13.77 g gypsum (0.08 mol) were suspended in 27.2 g water and stirred vigorously for 30 min. Next, 15 mL of the resulting suspension were hydrothermally treated in a 20 mL autoclave for 3 h at 180 °C. After cooling to ambient temperature, the paste obtained was removed from the autoclave and air-dried at 50 °C. X-ray powder diffraction confirmed that the product was pure $[Ca_4Al_2(OH)_{12}](SO_4) \cdot 12\, H_2O$ (see Fig. 6).

C_4AH_{13}, $[Ca_2Al(OH)_6](OH) \cdot 3\, H_2O$ was synthesized following the method described by Buttler et al. [22]. We modified their process by using C_3A and lime in water instead of anhydrous $CaO \cdot 2Al_2O_3$ (CA_2) in slightly undersaturated lime solution. Thus, 10.43 g C_3A (0.039 mol) and 2.80 g lime (0.05 mol) were suspended in 200 mL water and were left to react at 5 °C for at least 14 days in a closed bottle under careful exclusion of carbon dioxide. After centrifugation the precipitate was dried at ambient temperature under a nitrogen atmosphere in a desiccator over silica gel and pure C_4AH_{13} was obtained. Note that pure C_3A, suspended at room temperature in water, will react quantitatively within less than an hour to katoite (C_3AH_6), the thermodynamically stable hydration product of C_3A.

The comb structured PC superplasticizers of the methacrylic acid–*co*–ω-methoxy poly(ethylene glycole) methacrylate type were synthesized following a patent instruction [23]. The chemical structure of the PCs is presented in Fig. 2. Gel permeation chromatography (GPC) analysis of the synthesized polymers was performed using Waters 2695 Separation Module, Waters Ultrahydrogel™ 120, 250 and 500 separation columns, Waters 2787 Dual λ UV Absorbance Detector and Waters 2414 Refractive Index Detector. The eluent was 0.1 mol/L $NaNO_3$ at pH 12 (adjusted with NaOH). PC samples were measured in 1 wt.% aqueous solution and filtered through a 0.2 mm filter before the measurement. From GPC analysis, molar masses (M_w, M_n), polydispersity index and size of the dissolved polymers expressed by their hydrodynamic radius were obtained. The results are shown in Table 1.

The specific architecture of the synthesized polycarboxylate macromolecules was determined as well. Based on M_n obtained from GPC data and applying the procedure described in [4], the main chain length (MCL) of the PCs was calculated. The side chain length (SCL) of the PCs is known from the ester macromonomer used in the synthesis. Our PCs with side chains possessing 8.5 and 17 ethylene oxide units (EOUs)

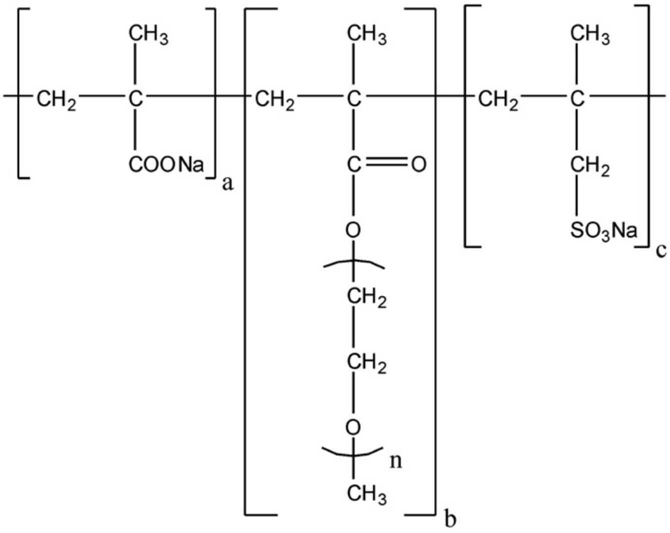

Fig. 2. Chemical composition of the synthesized PCs (a:b:c = 6:1:0.2); $n =$ number of ethylene oxide units.

Table 1
Molar masses (M_w, M_n), polydispersity index and hydrodynamic radius of the synthesized PC polymers.

Polymer	Molar mass M_w [Da]	Molar mass M_n [Da]	Polydispersity index (M_w/M_n)	Hydrodynamic radius R_h [nm]
8.5PC6	153,400	71,800	2.1	8.6
17PC6	135,600	26,640	5.1	10.5
45PC6	152,600	40,420	3.8	10.5
111PC6	110,200	40,830	2.2	8.9

exhibit a “worm-like” conformation, whereas the PC with 45 EOUs represents a polymer “brush” and the PC with 111 EOUs is a “star-like” polymer. A schematic drawing to scale of the PC structures is shown in Fig. 3. Obviously, the steric size of the synthesized PC polymers changes considerably from the PC possessing only 8.5 EOUs ($PC_{n=8.5}$) to the PC possessing 111 EOUs ($PC_{n=111}$).

2.2. Rehydration experiments

To begin with, rehydration of C_3A in the absence and presence of various amounts of sulfate was studied. For this purpose, C_3A was rehydrated in deionized water or dilute K_2SO_4 solution. The amount of K_2SO_4 added was varied to achieve SO_4^{2-}/C_3A molar ratios of 0, 0.1, 0.35, 0.7, 1 and 2. The respective amount of K_2SO_4 was dissolved in 100 mL of deionized water, and then 1 g C_3A was added to this solution showing a pH of about 11.7. The suspension was stirred at 75 °C for 48 h under argon, then centrifuged and the precipitate finally dried at 50 °C for 48 h in air in a drying oven. Under these conditions, no uptake of carbon dioxide was observed by XRD. The reaction temperature of 75 °C was chosen to obtain PC intercalates of higher crystallinity than at 20 °C, thus allowing better analysis by XRD. Additional experiments performed at 20 °C not shown here produced results with comparable tendency to those obtained at 75 °C.

Next, intercalation of PC in the absence of sulfate was studied by rehydration of C_3A in a diluted PC solution. The preparation method was similar to the synthesis we reported before [12,13]. In addition, intercalation in the presence of different amounts of sulfate was investigated. For this purpose, PC_n ($n_{EOU}=8.5, 17, 45$) was dissolved in 100 mL of deionized water at a concentration of 2.5 wt.-% and then, different amounts of K_2SO_4 were added to the PC_n solution according to the SO_4^{2-}/C_3A ratios mentioned in the sulfate experiments above. After stirring the PC solution with or without sulfate for 10 min, 1.0 g of C_3A was added and then left to react under protective argon atmosphere at 75 °C for 48 h. The precipitate was separated by centrifugation and washed with deionized water in order to remove residual polymer. The resulting solids were dried at 50 °C for 48 h in air in a drying oven. We observed that, when intercalation of PC occurs, the precipitate always consists of a gel-like layer on top and a compact layer at the bottom. The gel layer has a particularly high concentration of PC intercalates and therefore was used for intercalation analysis.

2.3. Anion exchange experiments

The potential for anion exchange between Ca–Al–A–LDH phases (calcium aluminum hydroxy hydrate, denominated as C_4AH_{13}, $[Ca_2Al(OH)_6](OH)\cdot 3\ H_2O$ and monosulfoaluminate, $[Ca_4Al_2(OH)_{12}](SO_4)\cdot 12\ H_2O$ and PC was studied by addition of PC solutions to aqueous suspensions of the Ca–Al–A–LDH phases. For the experiments, 1.5 g of Ca–Al–A–LDH ($A=OH^-$ or SO_4^{2-}) were added to 100 mL of a 2.5 wt.% PC solution in deionized water. This produces a white suspension with a pH of 11.7. The system was stirred under argon flow at 75 °C for 48 h, centrifuged and the precipitate was dried at 50 °C for 48 h in air in a drying oven.

2.4. Analytical methods

X-ray powder diffraction (XRD) patterns were obtained with a Bruker AXS D8 Advance diffractometer operating at 30 kV and 30 mA, using Cu-K_α radiation at $0.02°s^{-1}$ between 1.0° and 40° 2θ angles. C, H values were determined by conventional CHN analysis with a “elementar vario EL” apparatus from elementar Analysensysteme GmbH. S was measured with a “Euro EA” system from Hecatec. The Ca and Al contents were determined by analyzing dilute solutions of the synthesized compounds dissolved in concentrated HNO_3 utilizing induced coupled plasma atom emission spectrometry (ICP-AES). TOC analysis was carried out with a “high TOC II” from elementar Analysensysteme GmbH.

3. Results and discussion

3.1. Hydration of C_3A at different sulfate concentrations

To begin with, we examined the hydration products of C_3A in the absence and presence of various amounts of sulfate. The XRD powder diffractograms of the reaction products obtained at SO_4^{2-}/C_3A molar ratios between 0 and 2 are depicted in Fig. 4. In the absence of sulfate, C_3A is quantitatively transformed to katoite (C_3AH_6) within less than an hour. The small reflection denoted MC (monocarboaluminate or

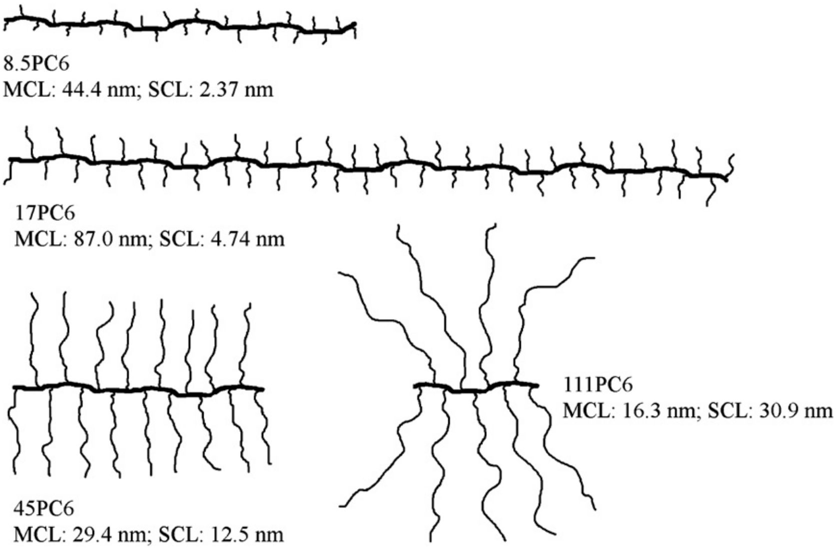

Fig. 3. Schematic representation of the polymer architecture for the synthesized PCs. (MCL = main chain length, SCL = side chain length).

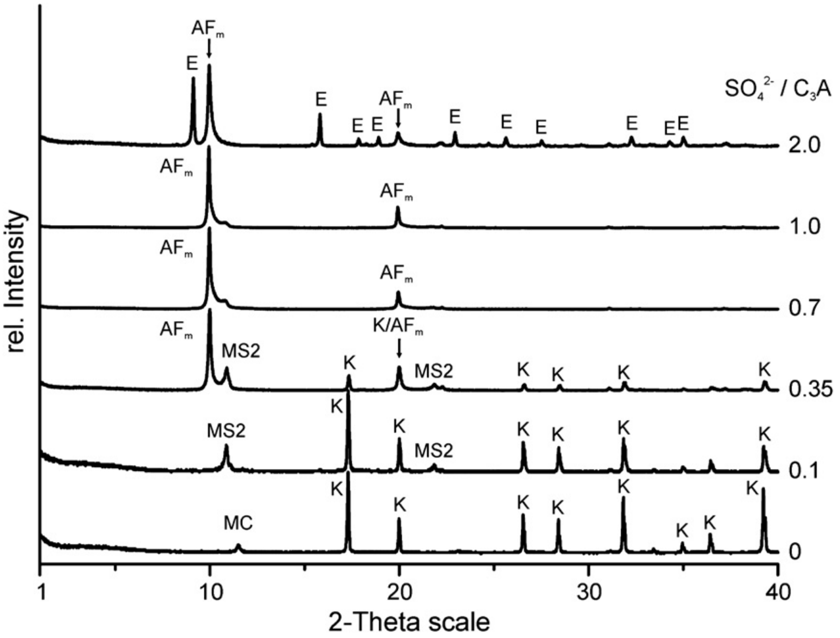

Fig. 4. Formation of different calcium sulfoaluminate hydrates during rehydration of C_3A at various sulfate/C_3A molar ratios (E = ettringite, $AF_m = [Ca_4Al_2(OH)_{12}](SO_4) \cdot 12\ H_2O$, $MS2 = [Ca_4Al_2(OH)_{12}](SO_4) \cdot 10\ H_2O$, K = katoite, $MC = [Ca_4Al_2(OH)_{12}](CO_3) \cdot 8\ H_2O$).

$[Ca_4Al_2(OH)_{12}](CO_3) \cdot 8\ H_2O)$ is an impurity which is formed through the uptake of carbon dioxide. At low molar ratios of SO_4^{2-}/C_3A (0.1 and 0.35), a sulfoaluminate containing only 10 mol of water (denominated "monosulfoaluminate 2", MS2 or $[Ca_4Al_2(OH)_{12}](SO_4) \cdot 10\ H_2O$) is formed besides katoite whereas regular monosulfoaluminate containing 12 mol of water (denominated AF$_m$ or $[Ca_4Al_2(OH)_{12}](SO_4) \cdot 12\ H_2O$) is present at a SO_4^{2-}/C_3A molar ratio of 0.35 and higher. With increasing SO_4^{2-}/C_3A molar ratio, the amount of katoite decreases until, at a molar ratio of 0.7, the reflections of katoite have entirely disappeared. This can be explained by the higher negative charge of sulfate in comparison with hydroxide: the sulfate anion has a greater tendency to intercalate into the Ca–Al–LDH phases. Therefore, katoite is not formed any longer when the sulfate content gets higher. Theoretically, a SO_4^{2-}/C_3A molar ratio of 0.75 is required to convert the entire amount of C_3A quantitatively to monosulfoaluminate. Further increase of the SO_4^{2-}/C_3A molar ratio to 2.0 results in a mixture of AF$_m$ phase and ettringite (AF$_t$ phase). This is to be expected, because at high sulfate concentrations ettringite is the thermodynamically more stable phase in comparison to AF$_m$ [24].

3.2. Hydration of C_3A in PC solution

Furthermore, (re)hydration of C_3A was studied in the presence of different PCs. XRD diffractograms show that for all PCs, a new reflection at low 2θ values appears, indicating a high basal spacing between the $[Ca_2Al(OH)_6]^+$ layers (Fig. 5). This confirms that intercalation of the PCs into the interlayer space of the Ca–Al–LDH phase has occurred. The d values of the newly formed organo-mineral phases increase steadily

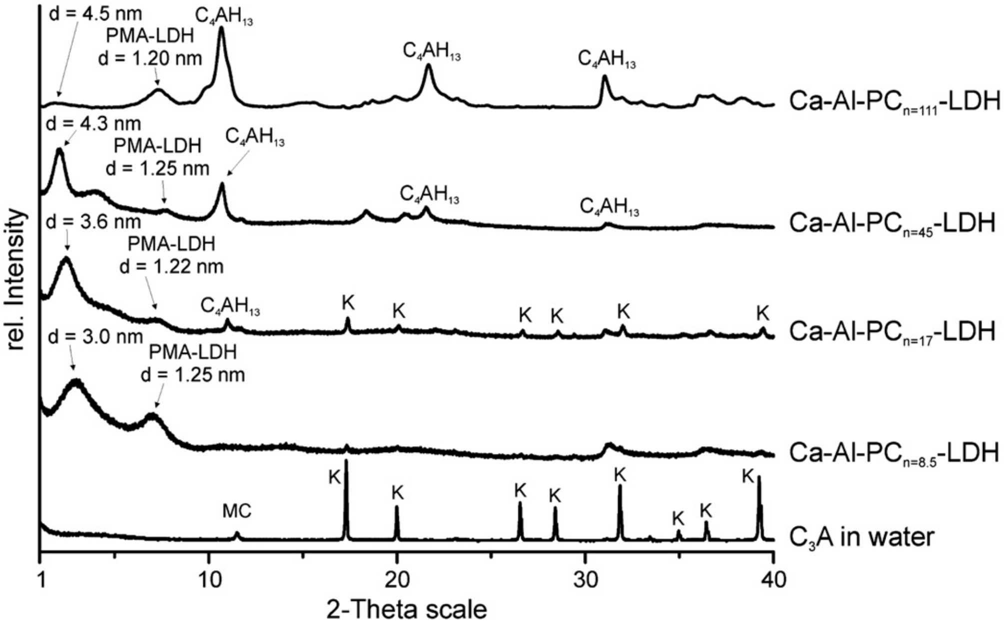

Fig. 5. XRD patterns of reaction products obtained from rehydration of C_3A in absence and presence of different PCs (K = katoite, $MC = [Ca_4Al_2(OH)_{12}](CO_3) \cdot 8\ H_2O$, PMA-LDH = polymethacrylate-LDH).

with increasing number of EOUs in the side chains: $d=3.0$ nm for $PC_{n=8.5}$, $d=3.6$ nm for $PC_{n=17}$, $d=4.3$ nm for $PC_{n=45}$ and $d=4.5$ for $PC_{n=111}$. The diffractograms shown in Fig. 5 suggest that with increasing side chain length, PC intercalation starts to decline while increasing amounts of C_4AH_{13} are being formed. This is highly obvious for $PC_{n=111}$ where only a small amount of Ca–Al–$PC_{n=111}$–LDH is detected. Instead, C_4AH_{13} is the main reaction product. Consequently, it can be concluded that in general, a limitation seems to exist for the steric size of PC to be intercalated. For our type of PC composed of methacrylic acid and MPEG methacrylate ester in a molar ratio of 6:1, intercalation appears to become difficult once the number of EOUs in the side chain exceeds approx. 100. It can be expected that for PCs possessing a lower amount of methacrylic acid and thus showing a higher side chain density, the number of EOUs preventing intercalation will be less than 100, due to the stronger steric effect of the side chains and the lower anionic charge of the host molecule.

At approx. 7° 2θ, another reflection with a *d* value of approx. 1.2 nm representing a small interlayer distance appears. At first, we could not assign this peak because all known AF_m phases including hydroxides, carbonates, chlorides, sulfates and mixtures thereof containing various amounts of water show different *d* values [8]. We then focused on anionic byproducts formed during polymerization or impurities present in the monomers which were used to synthesize the PCs. While methacrylic acid possesses a *d* value of 1.38 nm, for polymethacrylate Zn_2Al–LDH structures a *d* value of 1.24 nm has been observed [25]. Thus, it seems that minor amounts of polymethacrylate present in the non dialyzed PCs are extracted from solution and incorporated into LDH structures.

Intercalation of the PCs into the Ca–Al–LDH phase was also proven by elemental analysis. Based on the carbon content, the organic part of the organo-mineral phases was calculated (Table 2). The calculation method has been described before [12,13]. The organic parts of the intercalates lie between 21.4 and 53.9 wt.%, resp. Generally, the organic part increases with increasing side chain length of PC, except for $PC_{n=111}$. The lower organic part in the reaction product from this PC confirms that $PC_{n=111}$ intercalates less, as has already been observed in the XRD diffractograms (Fig. 5). Because of this poor intercalation ability, $PC_{n=111}$ was not used in the further experiments.

Once it was confirmed that PC intercalation generally is possible during rehydration of C_3A, we continued our study by investigating reactions of C_3A in simultaneous presence of both sulfate and PC. This system represents actual application conditions for PC in concrete.

3.3. Hydration of C_3A in presence of both sulfate and PC

When C_3A was hydrated in the presence of both PC and sulfate, the intercalation of all PCs was found to depend heavily on the amount of sulfate present in the reaction solution. In the following, the reaction of $PC_{n=45}$ will be discussed in detail as an example. All other PCs show similar behaviors than $PC_{n=45}$.

The XRD patterns of the reaction products formed from $PC_{n=45}$ at SO_4^{2-}/C_3A molar ratios between 0 and 2 are presented in Fig. 6. They clearly show that the hydration products change according to the amount of sulfate present during C_3A hydration. When no sulfate is present, the intercalation compound Ca–Al–$PC_{n=45}$–LDH possessing a *d* value of 4.3 nm is formed, as has been shown before (Fig. 5).

Table 2
Elemental analysis data of Ca–Al–PC_n–LDH intercalation compounds.

Ca–Al–PC–LDH intercalate	Ca [wt.%]	Al [wt.%]	C [wt.%]	H [wt.%]	Organic part [wt.%]
Ca–Al–$PC_{n=8.5}$–LDH	14.8	5.0	24.8	5.9	44.9
Ca–Al–$PC_{n=17}$–LDH	12.0	3.9	28.4	6.9	51.2
Ca–Al–$PC_{n=45}$–LDH	13.3	5.4	29.8	6.4	53.9
Ca–Al–$PC_{n=111}$–LDH	19.9	7.4	11.7	4.9	21.4

In the presence of low amounts of sulfate (SO_4^{2-}/C_3A molar ratios 0.1 and 0.35, resp.), the PC can still intercalate. The tendency to intercalate decreases, however, with increasing sulfate concentration. At a SO_4^{2-}/C_3A molar ratio of 0.7, intercalation of PC is no longer observed. Obviously, the ability of PC to intercalate depends on a low sulfate concentration present in the pore solution. It indicates that sulfate, because of its higher specific anionic charge density, has a higher tendency to occupy the interlayer space of Ca–Al–LDH phases than $PC_{n=45}$. Therefore, when enough sulfate is available to occupy all interlayer space, PC cannot intercalate at all. Consequently, the amount of free sulfate present during early cement hydration determines whether PC intercalation will occur or not.

Fig. 6 shows another interesting phenomenon which is occurring during PC intercalation at low sulfate concentrations. When the sulfate concentration increases (SO_4^{2-}/C_3A molar ratios of 0–0.35), the basal spacing of the resulting Ca–Al–$PC_{n=45}$–LDH compounds starts to increase from 4.3 nm (sulfate free system) to 4.8 nm ($SO_4^{2-}/C_3A=0.1$) and to 7.1 nm ($SO_4^{2-}/C_3A=0.35$). We attribute this effect to intersalation and/or interstratification of both $PC_{n=45}$ and potassium sulfate between the Ca–Al–LDH layers. Intersalation and interstratification are well known phenomena in the chemistry of layered compounds such as layered double hydroxides or clays [26,27]. Intersalation is the further uptake of cations and anions from salts (here: K_2SO_4) into the interlayer space, even if charge neutralization between the layers has been achieved before. The amount of salt intersalated between the main layers may vary. It can be significant and thus result in a markedly higher *d* value. Interstratification means that the interlayers are randomly filled with either sulfate or PC guest anions. Such LDH particles show a variation in the sequence of their layers. The *d* values of their *001* reflections shown in the XRD are an arithmetic average of all basal spacings and their relative frequency as they exist in the LDH particle. These peaks are typically quite broad and do not give a harmonic *00l* series. The strong increase in the *d* value of Ca–Al–$PC_{n=45}$–LDH from 4.3 to 7.1 nm and the relative sharpness of the *001* reflection point to intersalation of K_2SO_4 rather than interstratification as the cause for this phenomena. A schematic drawing of Ca–Al–PC_n–LDH structures intersalated with K_2SO_4 and interstratified with sulfate is shown in Fig. 7.

When sulfate is present, C_4AH_{13} no longer forms and is completely replaced by the thermodynamically more stable sulfoaluminate MS2. Further increase of the sulfate concentration up to a SO_4^{2-}/C_3A molar ratio of 2.0 causes the main peak of MS2 occurring at approx. 11° 2θ to become sharper and more intense, indicating a better periodic stacking of the Ca–Al–SO_4^{2-}LDH layers. The actual increase in intensity of this peak is not shown in Fig. 6, because all diffraction patterns were normalized to the most intense peak.

Interestingly, even at high sulfate concentrations no ettringite was detected. A possible explanation is that the PC present causes ettringite to form in an amorphous form. Thus, it is undetectable in XRD. It has been reported earlier that superplasticizers generally reduce the size of ettringite crystals, probably by surface adsorption [2]. Other researchers have observed that under certain conditions, essentially amorphous ettringite needles possessing only a very thin crystalline shell which is undetectable in XRD can be formed [28].

The results described above were also confirmed by elemental analysis. The data is shown in Table 3. The carbon and sulphur contents in the reaction compounds indicate whether intercalation has occurred or not.

According to Table 3, the carbon content (i.e. the organic part) of the reaction products decreases whereas the sulfate content increases. This indicates that, with increasing sulfate concentration in the pore solution, intercalation of the PC becomes more difficult, as has already been observed in the XRD patterns (Fig. 6). More specifically, at a SO_4^{2-}/C_3A molar ratio of 0.7, only a minor amount of PC has intercalated. At SO_4^{2-}/C_3A molar ratios ≥1, the organic content in the reaction product is less than 10 wt.%. Such values are typical for PC adsorption

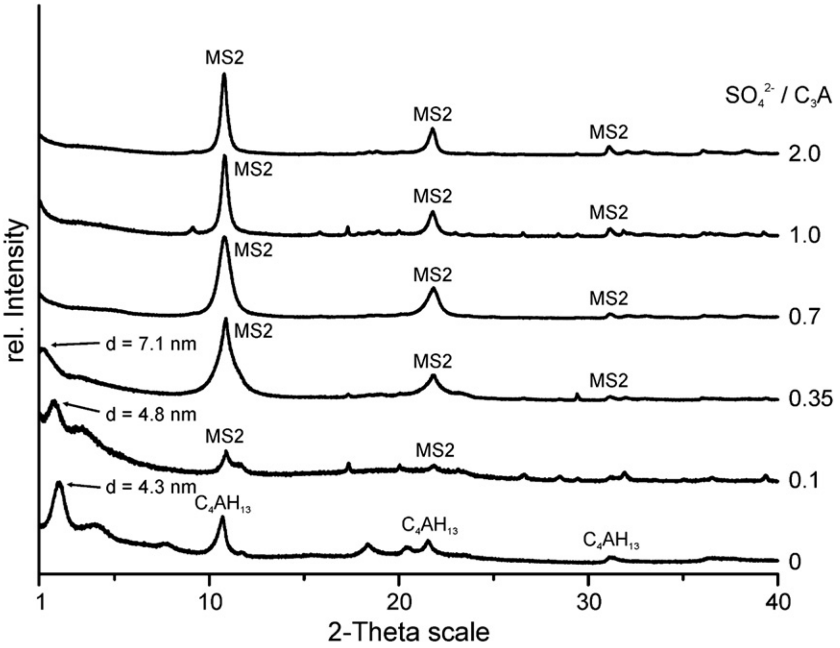

Fig. 6. XRD patterns of reaction products obtained from rehydration of C_3A in presence of 2.5 wt.% $PC_{n=45}$ and varying concentrations of sulfate ($MS2 = [Ca_4Al_2(OH)_{12}](SO_4) \cdot 10\ H_2O$).

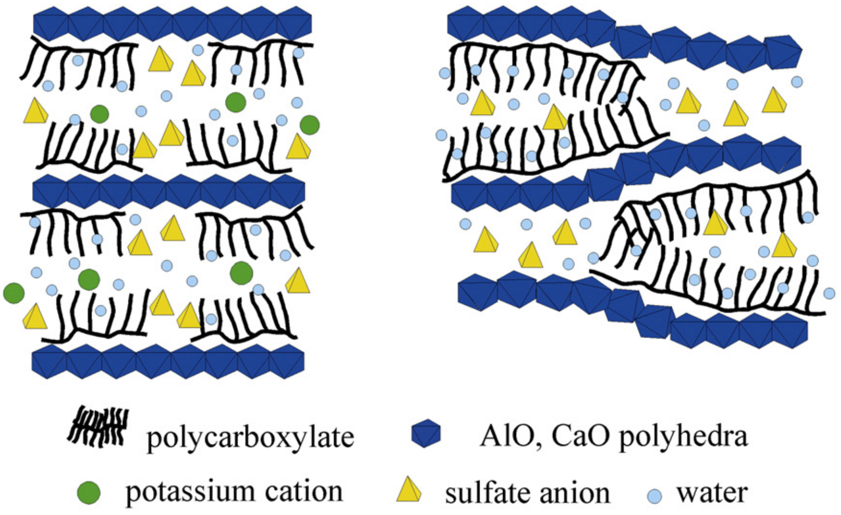

Fig. 7. Schematic illustration of Ca–Al–PC–LDH structures intersalated with K_2SO_4 (left) and interstratified with sulfate anions (right).

on the cationic surface of AF_m or AF_t particles [2]. They confirm that at SO_4^{2-}/C_3A molar ratios ≥1.0, PC does not intercalate any more, as has been shown before in the XRD patterns of Fig. 6. This result is also supported by the sulfate content of the C_3A reaction products (Table 3). The sulfate content increases with decreasing organic part, indicating that sulfate replaces PC in the interlayer. Note that the theoretical sulfate contents of monosulfoaluminate and MS2 are 15.6 and 16.5 wt.%, resp.

Table 3
Elemental analysis data of C_3A rehydration products in presence of $PC_{n=45}$ at different SO_4^{2-}/C_3A molar ratios.

SO_4^{2-}/C_3A molar ratio	Ca [wt.%]	Al [wt.%]	C [wt.%]	H [wt.%]	S [wt.%]	Organic part [wt.%]	Sulfate [wt.%]
0	13.3	5.4	29.8	6.4	–	–	–
0.1	16.2	5.9	28.7	5.9	0.5	52.1	1.5
0.35	17.9	6.1	21.6	5.4	1.9	39.2	5.8
0.7	24.1	7.9	8.6	4.3	3.8	15.7	11.3
1.0	24.5	9.0	4.4	3.7	3.7	8.0	11.1
2.0	26.0	9.2	4.2	3.6	4.9	7.6	14.5

Similar experiments as with $PC_{n=45}$ and different SO_4^{2-} concentrations were carried out with $PC_{n=8.5}$ and $PC_{n=17}$ as well. Table 4 and Figs. 8 and 9 show a comparison of the data obtained for the three polymers $PC_{n=8.5}$, $PC_{n=17}$ and $PC_{n=45}$ at SO_4^{2-}/C_3A molar ratios of 0.35 and 1, resp.

At a high SO_4^{2-}/C_3A molar ratio (1.0), none of the PCs tested intercalates well. In the XRD patterns, no peaks typical for PC intercalation are visible (Fig. 8). The organic contents of the reaction products indicate that surface adsorption and not intercalation is the main interaction between PC and the aluminate hydrate (Table 4). The slightly higher organic contents in the reaction products with $PC_{n=8.5}$ and $PC_{n=17}$ suggest that PCs possessing shorter side chains and higher specific anionic charge density can compete somewhat better against sulfate, but the effect is only marginal. The broad peaks for AF_m and MS2

Table 4
Elemental analysis data of C_3A rehydration products formed in presence of $PC_{n=8.5}$, $PC_{n=17}$ and $PC_{n=45}$ at SO_4^{2-}/C_3A molar ratios of 0.35 and 1.0, resp.

Polymer	Ca [wt.%]	Al [wt.%]	C [wt.%]	H [wt.%]	S [wt.%]	Organic part [wt.%]	Sulfate [wt.%]
SO_4^{2-}/C_3A molar ratio = 1.0							
$PC_{n=8.5}$	21.6	8.0	7.1	4.1	3.5	12.6	10.5
$PC_{n=17}$	24.1	8.1	7.1	4.2	3.7	12.7	11.2
$PC_{n=45}$	24.5	9.0	4.4	3.7	3.7	8.0	11.1
SO_4^{2-}/C_3A molar ratio = 0.35							
$PC_{n=8.5}$	18.4	6.8	17.5	5.0	1.5	31.1	4.5
$PC_{n=17}$	16.1	5.8	23.2	5.8	0.8	41.6	2.5
$PC_{n=45}$	17.9	6.1	21.6	5.4	1.9	39.2	5.8

at 11° 2θ in the diffractograms result from interstratification of sulfate and small amounts of randomly distributed organic polymer. For all PCs, the sulfate content of the samples is comparable (10.5–11.1 wt.%).

At a SO_4^{2-}/C_3A molar ratio of 0.35, the amount of sulfate present is not sufficient to convert all C_3A quanititatively into pure monosulfoaluminate. Thus, the PCs can intercalate. Accordingly, intercalation of $PC_{n=17}$ and $PC_{n=45}$ is obvious from their diffractograms shown in Fig. 9. $PC_{n=8.5}$ seems to be a special case here. For this PC, a peak possessing only very low intensity is visible. This does not necessarily mean that no intercalation has occurred, because even the intercalation peak for pure Ca–Al–$PC_{n=8.5}$–LDH was quite broad and low in intensity (Fig. 5). It can be expected to get even broader and weaker when interstratification with some sulfate occurs, which is the case here. Another indication for the interstratification of both sulfate and PC is the low intensity and broad appearance of the peaks for MS2 (Fig. 9). Apparently, the Ca–Al–$PC_{n=8.5}$–LDH is contaminated by some amount of interstratified sulfate and MS2 contains a minor amount of PC and/or K_2SO_4 which are interstratified or intersalated. We explain this observation as follows: at the beginning of C_3A rehydration, enough sulfate is present to form exclusively sulfoaluminate. With decreasing sulfate concentration, $PC_{n=8.5}$ starts to randomly intercalate into the MS2 structure, resulting in a broader peak. When the dissolved sulfate content is very low, the PC intercalate becomes the main reaction product. It incorporates the remaining sulfate

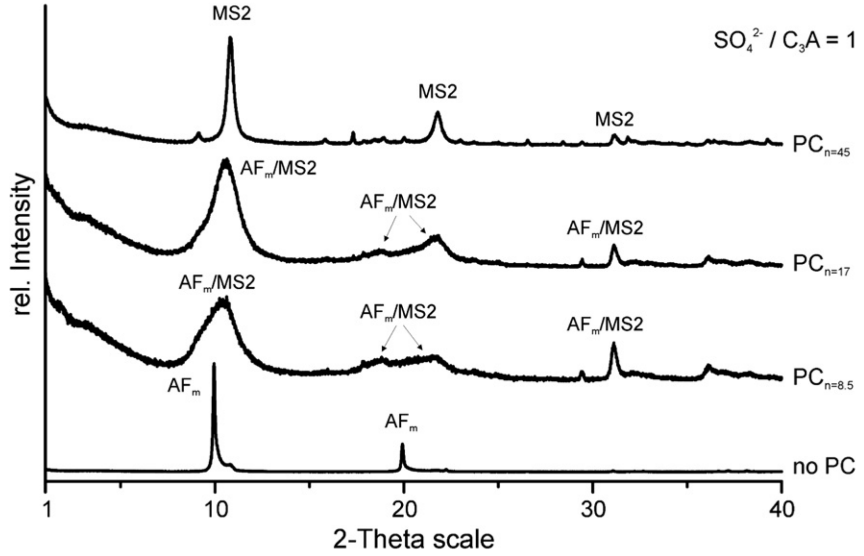

Fig. 8. XRD patterns of reaction products obtained from rehydration of C_3A in the presence of different PC_n ($n = 8.5$; 17 and 45) at a SO_4^{2-}/C_3A molar ratio of 1.0 ($AF_m = [Ca_4Al_2(OH)_{12}](SO_4) \cdot 12\ H_2O$, $MS2 = [Ca_4Al_2(OH)_{12}](SO_4) \cdot 10\ H_2O$).

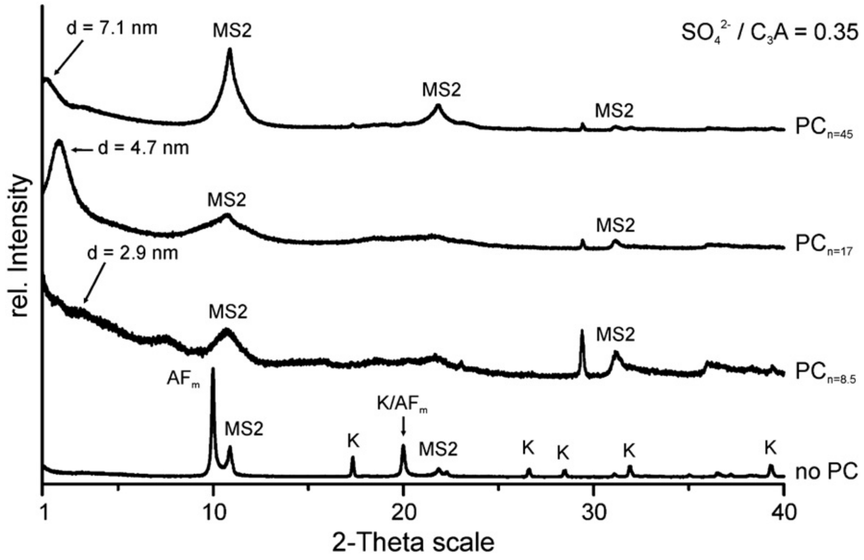

Fig. 9. XRD patterns of reaction products obtained from rehydration of C_3A in the presence of different PC_n ($n = 8.5$; 17 and 45) at a SO_4^{2-}/C_3A molar ratio of 0.35 ($AF_m = [Ca_4Al_2(OH)_{12}](SO_4) \cdot 12\ H_2O$, $MS2 = [Ca_4Al_2(OH)_{12}](SO_4) \cdot 10\ H_2O$, K = katoite).

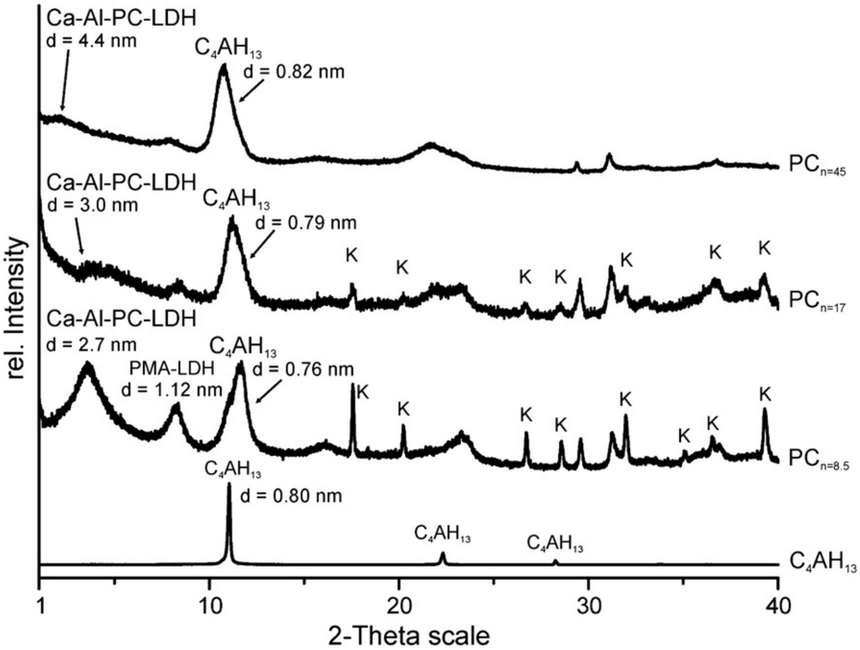

Fig. 10. XRD patterns of products obtained from anion exchange between C_4AH_{13} and different PCs (K = katoite, PMA-LDH = polymethacrylate-LDH).

anions. The result is an interstratified structure, best described as Ca–Al–$(PC_{n=8.5})_x$–$(SO_4^{2-})_y$–LDH, where $x >> y$. It can be expected that the initial intercalation process for sulfate occurs very fast whereas during intercalation of PC, the kinetics of the stacking process slows down. This is supported by the organic and sulfate contents found for these samples. The organic contents lie between 31 and 42 wt.%, resp. and are about 30% less than those for the pure Ca–Al–PC_n–LDH phases (Table 2). Additionally, the samples were found to contain smaller amounts of sulfate which can be ascribed to the second product MS2.

The present data lead to the conclusion that, when a sufficient amount of sulfate is present during rehydration of C_3A, no or only negligible amounts of PC intercalate. When less than the amount of sulfate necessary to quantitatively form monosulfoaluminate is present, much PC can intercalate. Therefore, the intercalation of PC into C_3A hydration products fully depends on the amount of dissolved sulfate present in the system.

3.4. Anion exchange between Ca–Al–A–LDH (A = OH^- and SO_4^{2-}) and PC

In the previous experiments, direct intercalation of PC during C_3A hydration was studied. However, intercalation may also occur as the result of an indirect formation process in which primary hydration products, namely hydroxy or sulfate layered calcium aluminum hydrates, undergo a subsequent anion exchange with PC. Therefore, the stability of Ca–Al–A–LDH phases (A = OH^- and SO_4^{2-}) in the presence of PC was studied by performing anion exchange experiments. For this purpose, freshly prepared C_4AH_{13} or monosulfoaluminate were added to an aqueous PC_n solution, stirred at 75 °C for 48 h and the precipitate was analysed. The results are shown in Figs. 10 and 11.

C_4AH_{13} undergoes anion exchange with all three PCs tested, as is shown in the XRD patterns of Fig. 10. The exchange is particularly strong for $PC_{n=8.5}$ and decreases with increasing side chain length. The organic content of the reaction products also confirms that

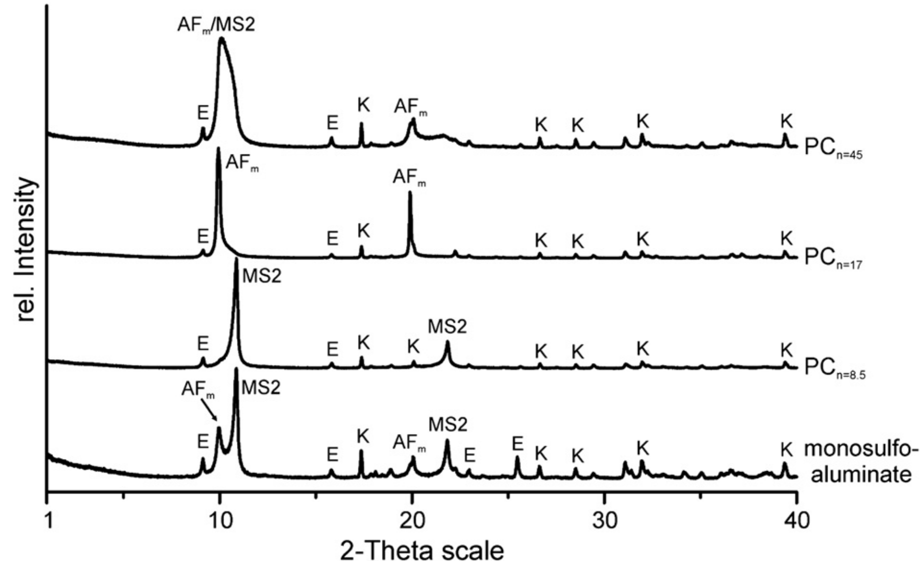

Fig. 11. XRD patterns of reaction products obtained from anion exchange between monosulfoaluminate and different PCs (E = ettringite, $AF_m = [Ca_4Al_2(OH)_{12}](SO_4) \cdot 12\ H_2O$, $MS2 = [Ca_4Al_2(OH)_{12}](SO_4) \cdot 10\ H_2O$, K = katoite).

Table 5
Elemental analysis data of products obtained from anion exchange between C_4AH_{13} and PC_n.

Polymer	C [wt.%]	H [wt.%]	Organic part [wt.%]
$PC_{n=8.5}$	17.6	4.9	31.4
$PC_{n=17}$	16.3	5.1	29.4
$PC_{n=45}$	19.7	5.3	35.8

Table 6
Elemental analysis data of products obtained from anion exchange between monosulfoaluminate and PC_n.

Polymer	C [wt.%]	H [wt.%]	S [wt.%]	Organic part [wt.%]	Sulfate part [wt.%]
$PC_{n=8.5}$	1.9	3.5	3.9	3.4	11.7
$PC_{n=17}$	2.2	3.8	2.4	4.0	7.3
$PC_{n=45}$	2.9	3.7	3.5	5.2	10.5

intercalation has occurred (Table 5). The *d* values found for the PC intercalates correspond well with the *d* values for the pure Ca–Al–PC–LDH phases prepared by rehydration of C_3A in the presence of PC_n (Fig. 5). The broad appearance of the C_4AH_{13} peak at approx. 11° 2θ and of the Ca–Al–PC_n–LDH peak indicates an incomplete exchange of OH^- against PC anions. Obviously, the reaction compounds exhibit considerable interstratification. The coexistence of both C_4AH_{13} and Ca–Al–PC_n–LDH phases after 48 h reaction time also indicates that the exchange kinetics is quite slow. Interestingly, only small amounts or no katoite at all is formed during the anion exchange. Apparently, C_4AH_{13} is stabilized by the PCs. They prevent the conversion into katoite. Furthermore, the XRD patterns of all anion exchange products show that minor amounts of polymethacrylate contained in the PC solutions have incorporated as well and form additional LDH structures (also see Fig. 5). This reaction is especially observed for $PC_{n=8.5}$.

Next, the anion exchange between Ca–Al–SO_4–LDH (monosulfoaluminate) and PCs was studied. The XRD patterns of the reaction products are shown in Fig. 11. Obviously, for all PCs no new reflections at low 2θ angles appear, indicating that no anion exchange and thus no PC intercalation took place. Instead, all reflections can be assigned to AF_m, MS2 and the byproducts ettringite and katoite. The carbon contents in these products were 3.4 wt.% for $PC_{n=8.5}$, 4.6 wt.% for $PC_{n=17}$ and 5.2 wt.% for $PC_{n=45}$ (Table 6). These low numbers prove that the PCs are merely adsorbed on the surface of the sulfoaluminates and are not intercalated. At the same time, a relatively high sulfate content was found.

The anion exchange experiments allow to conclude that sulfate, because of its higher anionic charge density, is so strongly bound in between the Ca–Al–LDH layers that PCs cannot replace it whereas hydroxide anions can be exchanged over time. Thus, C_4AH_{13} formed in undersulfated cements as primary hydration product, can still allow intercalation of PC over time. This is impossible when monosulfoaluminate is the primary AF_m phase.

3.5. Anion exchange between Ca–Al–PC–LDH and SO_4^{2-} or OH^-

In the first experiment, pure Ca–Al–PC_n–LDH phases synthesized by rehydration of C_3A in PC solution as described before were subjected to anion exchange with sulfate anions by suspending them in aqueous sulfate solutions.

The solution contained a sulfate amount equivalent to 100% anion exchange capacity (aec) of the Ca–Al–PC_n–LDH phase. The aec was calculated based on the composition of the pure phases as shown in Table 2, assuming that for each Al present in the main layer, 0.5 mol of SO_4^{2-} are necessary to achieve complete anion exchange. K_2SO_4 was used as source for sulfate. Reaction conditions were 2 h stirring at room temperature. Afterwards, the suspension was centrifuged and the supernatant was used for TOC measurement. Fig. 12 shows the XRD patterns of the products.

After 2 h of reaction time, considerable replacement of PC by the sulfate ion is observed. The d values of the diffraction peaks of the PC intercalates show lower intensity and have become broader than for the pure phases (Fig. 5). This is typical for incomplete ion exchange. At the same time, the reflections which previously were ascribed to polymethacrylate-LDH (*d* value 1.12 nm) are still observed. This is particularly the case for $PC_{n=8.5}$. Thus, it seems that because of their high anionic charge, polymethacrylate-LDHs are more stable against sulfate than PC–LDHs. Therefore, they undergo less anion exchange than PC.

Based on the organic contents found in the supernatant, the percentage of PC_n exchanged by sulfate was calculated and found as follows: 11.9 wt.% for $PC_{n=8.5}$, 27.9 wt.% for $PC_{n=17}$ and 64.6 wt.% for $PC_{n=45}$. This shows that $PC_{n=45}$ is exchanged from the interlayer space by sulfate to a much greater extent than $PC_{n=17}$ or $PC_{n=8.5}$. This is consistent with the observation that in the diffractograms of the reaction products of Ca–Al–$PC_{n=8.5}$–LDH and Ca–Al–$PC_{n=17}$–LDH (Fig. 12), no monosulfoaluminate is detected. The different behavior of the PCs is explained by their different specific anionic charge density, which is highest for $PC_{n=8.5}$ and

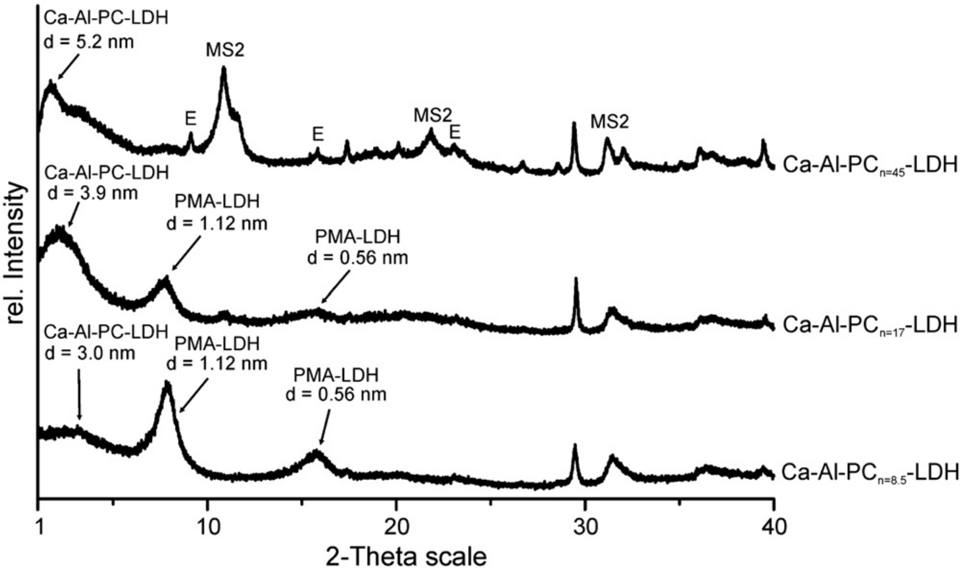

Fig. 12. XRD patterns of reaction products obtained from anion exchange between Ca–Al–PC_n–LDH and sulfate; sulfate concentration was at 100% anion exchange capacity, calculated on PC part contained in Ca–Al–PC_n–LDH (E = ettringite, MS2 = $[Ca_4Al_2(OH)_{12}](SO_4) \cdot 10\ H_2O$, PMA-LDH = polymethacrylate-LDH).

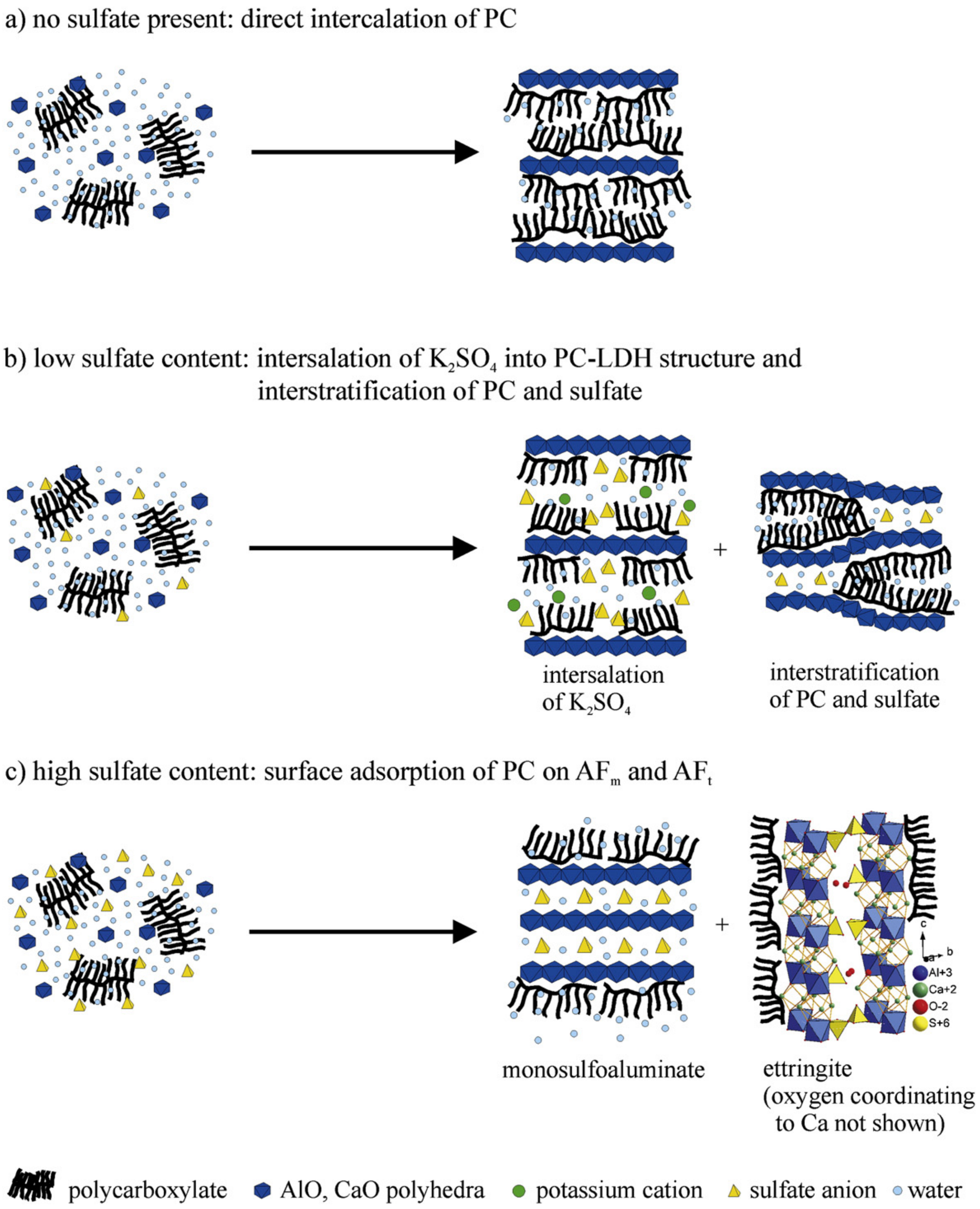

Fig. 13. Illustration of potential interactions between C_3A and PC during rehydration of C_3A as a function of sulfate content present in the cement pore solution.

lowest for $PC_{n=45}$. Therefore, $PC_{n=8.5}$ can compete much better against sulfate than $PC_{n=17}$ or $PC_{n=45}$.

These results are very well suited to illustrate a basic rule for the intercalation process: When several guest anions are present, the system reaches an equilibrium through exfoliation and restacking in which the anion with the highest charge density is intercalated in between the cationic host layers. Only after this prime compound has been consumed quantitatively, less anionic guest molecules have a chance to be incorporated, provided there is still enough C_3A available for the formation of LDH compounds. The anion with the lowest negative charge will remain in solution. Our experiments allow to conclude that the specific anionic charges of the guest molecules present are as follows: $SO_4^{2-} > \text{polymethacrylate} > PC_n$.

Additionally, anion exchange experiments between Ca–Al–PC–LDH and OH^- ions from $Ca(OH)_2$ and NaOH, resp. were carried out at pH 12.8 and under the same conditions as for sulfate. The XRD patterns of the reaction products not shown here only exhibit a broadening of the *001* reflections, indicating lower crystallinity and uptake of various amounts of water into the Ca–Al–PC_n–LDH interlayer. Elemental analysis showed that the organic part in the reaction products decreased only by 5 wt.% for $PC_{n=17}$ and $PC_{n=45}$, resp. and by 13 wt.% for $PC_{n=8.5}$. Again, this confirms that not much PC is exchanged by OH^-. Obviously, the charge density of the OH^- anion is too low to replace the PC polymer in the LDH compound. This result was confirmed by elemental analysis for the exchange products. Their carbon contents were comparable with the contents found for the starting materials (Table 2). The fact that PC–LDH phases do not exchange with OH^- is not surprising. They were synthesized in alkaline solution (pH 11.7) over a reaction time of 2 d. This indicates that the Ca–Al–PC_n–LDH phases are thermodynamically more stable than Ca–Al–OH–LDH phases. Thus, OH^- cannot be expected to exchange the polymer from the PC intercalates.

The behavior of PCs as observed in the anion exchange experiments with sulfate might play an important role for their application in undersulfated, C_3A rich cements. There, initially formed calcium aluminate hydrates may be transformed into organo-mineral phases through gradual intercalation of PC by exchange of the OH^- anion.

4. Mechanisms for PC intercalation into C_3A hydrates

Based on the results discussed above, we can now draw general schemes for the interaction of PCs with C_3A. This interaction strongly depends on the concentration of sulfate present. The different possibilities are illustrated in Figs. 13 and 14.

First, there are two direct routes for the formation of PC intercalates (Fig. 13). Both are based on rehydration of C_3A. When C_3A hydrates in the presence of PC and at zero or low SO_4^{2-} concentration, intercalation of PC or interstratification of both PC and SO_4^{2-} occurs. The PC intercalate may also contain some amount of alkali sulfate which becomes intersalated into the PC–LDH structure. Additionally, PC will adsorb on the positive surfaces of the PC–LDH particles. However, intercalation of PC will not take place at all when C_3A hydrates at high SO_4^{2-} concentrations. In this case, the thermodynamically more stable monosulfoaluminate and ettringite will be formed (Fig. 13(c)). Once monosulfoaluminate or ettringite have been formed, PC can only adsorb onto the cationic surface of the AF_m and AF_t particles, as has been shown before [2]. Intercalation is no longer possible.

In addition, an indirect formation pattern exists. In undersulfated cements (i.e. those with SO_4^{2-}/C_3A molar ratios below or equal to 0.35 where SO_4^{2-} presents the concentration of sulfate dissolved immediately upon contact of cement with water, and C_3A presents the amount of aluminate exposed on the surface of the cement grain), hydration of the aluminate phase produces C_4AH_{13} or C_2AH_8. There, through exchange of the weakly bound hydroxide interlayer anion, PC can still intercalate (Fig. 14(a)). This exchange, however, is slow and only partial. Therefore, this second mechanism of formation will not lead to a major consumption of PC. When monosulfoaluminate is the main hydrate phase formed from C_3A hydration, PC will only adsorb onto the AF_m surface, while no intercalation is possible (Fig. 14(b)).

5. Conclusions

The formation of PC intercalation compounds can occur via two completely different mechanisms: First, in a direct synthesis between hydrating C_3A and PC, and second, through an indirect process involving calcium aluminate hydrates (Ca–Al–OH–LDH phases) as precursors which undergo anion exchange with PC in releasing initially intercalated OH^- anions. However, no matter which mechanism prevails, intercalation is generally possible only in undersulfated systems where the amount of quickly soluble sulfate present in cement is less than required to quantitatively convert all C_3A present to monosulfoaluminate and/or ettringite.

a) C_4AH_{13}: partial exchange of OH^- against PC

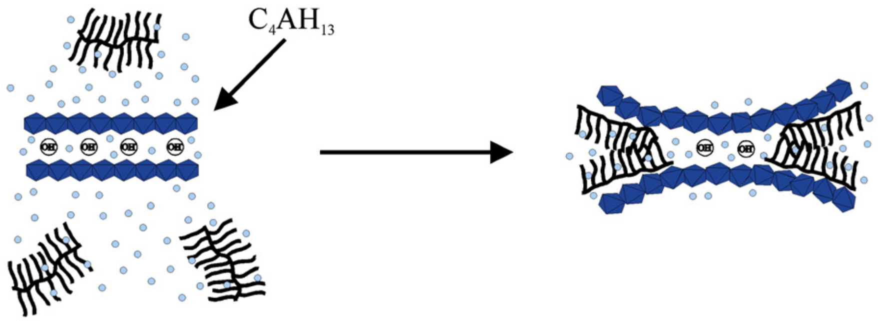

b) monosulfoaluminate: surface adsorption of PC

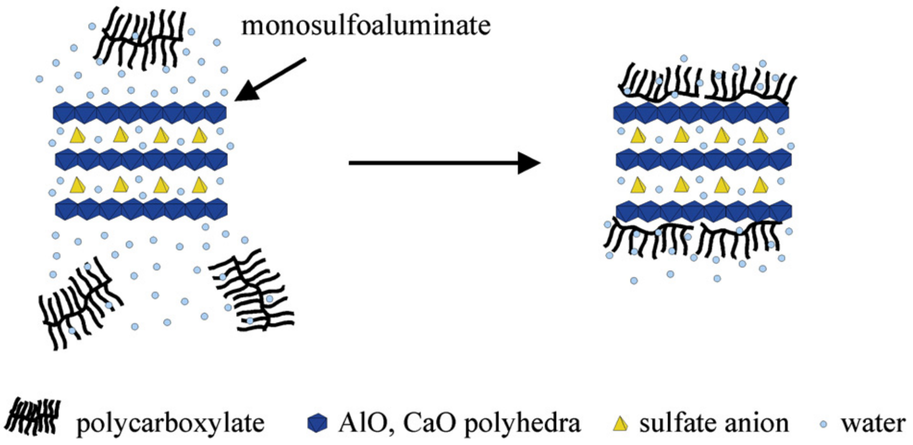

Fig. 14. Illustration of interaction possibilities between AF_m phases formed at low sulfate concentrations in the cement pore solution and PC.

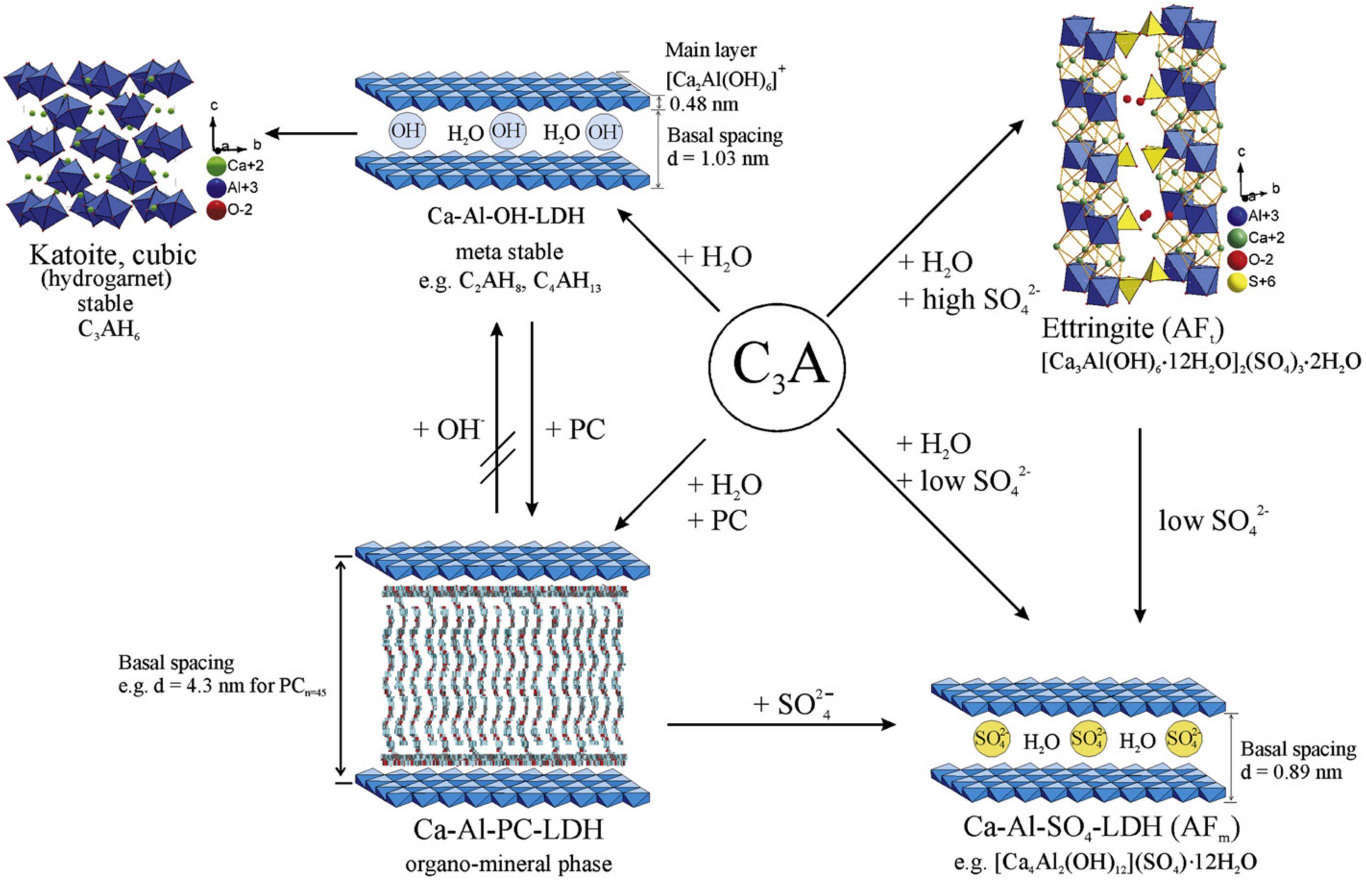

Fig. 15. Schematic representation of potential reaction patterns of C_3A hydrating at different SO_4^{2-} concentrations and in presence and absence of PC superplasticizer.

At 75 °C, the composition of the PC-organo-mineral phases may vary with the reaction conditions. PC–LDH compounds formed in essentially sulfate free systems may contain some interstitial hydroxide anions as well. This is particularly expected for PCs possessing a low specific anionic charge density or for PCs which, because of steric reasons, cannot achieve complete charge compensation between the cationic layers. In the presence of sulfates, the SO_4^{2-} anion can interstratify for the same reason. Additionally, PC–LDH structures with intersalated salts (e.g. alkali sulfates) are possible. Thus, the family of LDH structures containing PC which are potentially formed in cement is represented by the general formula $[Ca_2Al(OH)_6][(PC)_a(OH)_b(SO_4)_c(M^I_2SO_4)_d]\cdot z\ H_2O$, where the total negative charge achieved by the anions PC, hydroxide and sulfate is −1.

Based upon these findings, we can now draw a more complete reaction scheme for C_3A hydrating at different sulfate concentrations and in the presence and absence of PC. The various possibilities leading to different inorganic as well as organo-mineral compounds are summarized in Fig. 15. Obviously, the interaction between C_3A and PC is quite complex. Surface adsorption of PC on AF_m and AF_t phases will always occur because of the positive surface charge of these hydrates [2], whereas the intercalation potential is determined by the amount of sulfate present in the cement and the steric size of PC.

The study of PC intercalation is of great importance for the application of these superplasticizers in concrete and mortar. In experiments reported elsewhere, we could demonstrate that in a paste prepared from an undersulfated cement under conditions which are typical for concrete, PC-organo-mineral phases are formed. These results confirm our principle findings described here. Generally, PC intercalation is an unwanted process because it can lead to higher dosages of these expensive admixtures. Additionally, it is thought to be responsible for the sometimes huge differences in concrete flowability obtained at early and delayed PC addition [29]. Obviously, a great variety of cements is produced and used in concrete. Some of them are undersulfated and thus are more prone to PC intercalation. It is unlikely that cement manufacturers will adjust their products to prevent intercalation. Instead, the use of PC admixtures with longer side chains and lower anionic charge density which are less susceptible to form organo-mineral phases appears to be a potential solution to minimize the negative effects of intercalation. These PC molecules should be less sensitive to differently sulfated cements. They can be expected to be more robust in their application.

This work demonstrates the principle mechanisms resulting in the formation of PC organo-mineral phases during C_3A hydration. The authors acknowledge that some of the conditions chosen here such as the reaction temperature and time, and the absence of other phases and surplus ions (e.g. Ca^{2+}) are different from the usual conditions in cement and concrete. Based upon this fundamental study, the reaction possibilities existing in actual concretes or mortars can be studied now. Further studies will be needed to understand the consequences of PC intercalation with respect to product performance better. From a chemical point of view, it would be interesting to know the steric orientation of PC intercalated in between the cationic $[Ca_2Al(OH)_6]^+$ main layers.

References

[1] V.S. Ramachandran, Superplasticizers, Progr. Cement Concr. 1 (1992) 345–375.
[2] J. Plank, C. Hirsch, Superplasticizer Adsorption on Synthetic Ettringite, 2003, pp. 283–297, SP-217.
[3] A. Ohta, T. Sugiyama, Y. Tanaka, Fluidizing mechanism and application of polycarboxylate-based superplasticizers, 5th CANMET/ACI International Conference on Superplasticizers and Other Chemical Admixtures in Concrete, SP-173, 1997, pp. 359–378.
[4] A. Ohta, T. Sugiyama, T. Uomoto, Study of dispersing effects of polycarboxylate-based dispersant on fine particles, 6th CANMET/ACI International Conference on Superplasticizers and Other Chemical Admixtures in Concrete SP-195, 2000, pp. 211–227.
[5] J. Plank, D. Vlad, A. Brandl, P. Chatziagorastou, Colloidal chemistry examination of the steric effect of polycarboxylate superplasticizers, Cement Int. 3 (2005) 100–110.

[6] K. Yamada, S. Ogawa, S. Hanehara, Controlling of the adsorption and dispersing force of polycarboxylate-type superplasticizer by sulfate ion concentration in aqueous phase, Cem. Concr. Res. 31 (2001) 375–383.

[7] K.L. Scrivener, P.L. Pratt, Microstructural studies of the hydration of C3A and C4AF independently and in cement paste, Proc. Br. Ceram. Soc. 35 (1984) 207–219.

[8] H.F.W. Taylor, Cement Chemistry, Second ed., Thomas Telford Ltd, London, 1997, p. 480.

[9] P. Meredith, A.M. Donald, N. Meller, C. Hall, Tricalcium aluminate hydration: microstructural observations by in-situ electron microscopy, J. Mater. Sci. 39 (2004) 997–1005.

[10] V. Fernon, A. Vichot, N. Le Goanvic, P. Colombet, F. Corazza, U. Costa, Interaction Between Portland Cement Hydrates and Polynaphthalene Sulfonates, 1997, pp. 225–248, SP-173.

[11] L. Raki, J.J. Beaudoin, L. Mitchell, Layered double hydroxide-like materials: nanocomposites for use in concrete, Cem. Concr. Res. 34 (2004) 1717–1724.

[12] J. Plank, Z. Dai, P.R. Andres, Preparation and characterization of new Ca–Al-polycarboxylate layered double hydroxides, Mater. Lett. 60 (2006) 3614–3617.

[13] J. Plank, H. Keller, P.R. Andres, Z.M. Dai, Novel organo-mineral phases obtained by intercalation of maleic anhydride-allyl ether copolymers into layered calcium aluminum hydrates, Inorg. Chim. Acta 359 (2006) 4901–4908.

[14] R. Allmann, Die Doppelschichtstruktur der plättchenförmigen Calcium-Aluminium-Hydroxisalze am Beispiel des $3CaO \cdot Al_2O_3 \cdot CaSO_4 \cdot 12H_2O$, N. Jb. Miner. Mh. (1968) 140–144.

[15] G. Brown, M.C. Gastuche, Mixed magnesium aluminium hydroxides. II. Structure and structural chemistry of synthetic hydrocarbonates and related minerals and compounds, Clay Miner. 7 (1967) 193–201.

[16] F. Leroux, P. Aranda, J.P. Besse, E. Ruiz-Hitzky, Intercalation of poly(ethylene oxide) derivatives into layered double hydroxides, Eur. J. Inorg. Chem. (2003) 1242–1251.

[17] N.T. Whilton, P.J. Vickers, S. Mann, Bioinorganic clays: synthesis and characterization of amino- and polyamino acid intercalated layered double hydroxides, J. Mater. Chem. 7 (1997) 1623–1629.

[18] C.O. Oriakhi, I.V. Farr, M.M. Lerner, Incorporation of poly(acrylic acid), poly(vinylsulfonate) and poly(styrenesulfonate) within layered double hydroxides, J. Mater. Chem. 6 (1996) 103–107.

[19] J.M. Oh, S.Y. Kwak, J.H. Choy, Intracrystalline structure of DNA molecules stabilized in the layered double hydroxide, J. Phys. Chem. Solids 67 (2006) 1028–1031.

[20] D. Stephan, P. Wilhelm, Synthesis of pure cementitious phases by sol–gel process as precursor, Z. Anorg. Allg. Chem. 630 (2004) 1477–1483.

[21] A. Tomisaburo, I. Kazuto, M. Takeru, T. Kouichi, Verfahren zur Herstellung von Calciumaluminatmonosulfat-hydrat, 1976 Germany, DE2551310.

[22] F.G. Buttler, L.S.D. Glasser, H.F.W. Taylor, Studies on 4CaO*Al2O3*13H2O and the related natural mineral hydrocalumite, J. Am. Ceram. Soc. 42 (1959) 121–126.

[23] M. Kinoshita, K. Okada, M. Iida, Water-Soluble Vinyl Polymer-Based Dispersants for Cement and Method for Producing Concrete Using the Dispersants, 1999 Japan, 99-301578 940374, 19990303.

[24] F.W. Locher, Cement. Principles of Production and Use, Vbt Verlag Bau U. Technik, Düsseldorf, 2006, p. 535.

[25] A. Aguzzi, V. Ambrogi, U. Costantino, F. Marmottini, Intercalation of acrylate anions into the galleries of Zn–Al layered double hydroxide, J. Phys. Chem. Solids 68 (2007) 808–812.

[26] G.S. Thomas, P.V. Kamath, Line broadening in the PXRD patterns of layered hydroxides: the relative effects of crystallite size and structural disorder, J. Chem. Sci. 118 (2006) 127–133.

[27] H. van Olphen, An Introduction to Clay Colloid Chemistry, second ed., Wiley-Interscience, New York, 1977, p. 318.

[28] H. Pöllmann, Building materials mineralogy — methods and characterization of phases during the hydration of cements, Oral Presentation at Building Materials Workshop, 2009, Halle.

[29] R.J. Flatt, Y.F. Houst, A simplified view on chemical effects perturbing the action of superplasticizers, Cem. Concr. Res. 31 (2001) 1169–1176.